RECONSTRUCTING THE CHRONOLOGY OF BUILDING THE SOUTHWEST CHURCH OF UMM EL-JIMAL, JORDAN BY AMS RADIOCARBON DATING OF MORTAR AND PLASTER

Khaled Al-Bashaireh*

Department of Archaeology, Yarmouk University, Postal Code 211-63, Irbid, Jordan

ABSTRACT. The research aims to reconstruct the chronology of building the Southwest Church, Umm el-Jimal, Jordan by AMS radiocarbon dating organic inclusions uncovered from the mortars collected from the floor of the church, seat of the apse and the base of the north wall. It sheds light on the major aspects of mortar recipes at the time of their production. Samples were examined macroscopically with magnifying lenses and characterized using archaeometric techniques of optical microscopy and X-ray diffraction. The radiocarbon dates showed that 594–643 AD is the most probable age for flooring and plastering the church and 995–1154 AD is the earliest possible date for its final collapse. The preparatory layers of the church floor were laid on an older one, probably of a yard, and its north wall was raised on an older base, both most probably date to the late fifth–early sixth century AD. The production recipe of the mortars is made from a lime binder and inclusions mainly of organic (charcoal) and inorganic (quartz, grog, volcanics). The mortars have the same recipe regardless their bedding and jointing functions which remained unchanged during the building stages of church complex.

KEYWORDS: AMS radiocarbon, chronology reconstruction, mortar, production technology, Southwest Church, Umm el-Jimal.

INTRODUCTION

The Umm el-Jimal archaeological site is located in northern Jordan, in the semi-arid basaltic plateau which covers the northeastern part of Jordan, near the border with Syria, and on a side-road joining the *Via Nova Traiana* which passes about 6 km to the west of the site. Umm el-Jimal, which has an unknown ancient name (De Vries 1994), belonged to the bishopric of Bostra situated few kilometers north of it (Figure 1). It is considered the most important of the archaeological sites in east Jordan built with black basalt stones by corbelling techniques.

The Umm el-Jimal site was settled by the Nabateans, Romans, Byzantines and Umayyads from the first century AD to the eighth century AD. After its destruction, mainly by the disastrous earthquake of 749 AD, it was abandoned until the twentieth century AD, when Druze and Arab nomads moved into the site and repaired and modified many houses and reservoirs for their domestic use (De Vries 1979). The Druze left the site during the 1930s, while the Masa'ed tribe left it during the early 1970s.

The site started to grow with the construction of military structures (gates, city wall, military forts) during the early and late Roman period (63 BC–324 AD), while it was converted to domestic and commercial uses with reduced military presence during the early Byzantine period, 324–490 AD, specifically the fifth century AD (De Vries 1985; Glueck 1942; Al-Shorman et al. 2017). It prospered during the late Byzantine period (490–636 AD) where it witnessed a peak in the construction of houses, reservoirs, churches, etc. and its population reached its zenith. Prosperity continued during the Umayyad period, where maintenance and renovation of many structures took place (De Vries 1985:251).

The city is distinguished by its large number (16) of churches (Figure 2) identified during the surveys and excavations conducted at the site in the past decades (Butler 1913; De Vries 1990, 1998). The churches were named based on their location in the site (West Church, North Church, Southwest Church, etc.), their size (Cathedral, Chapel Outside East Wall, etc.),

---

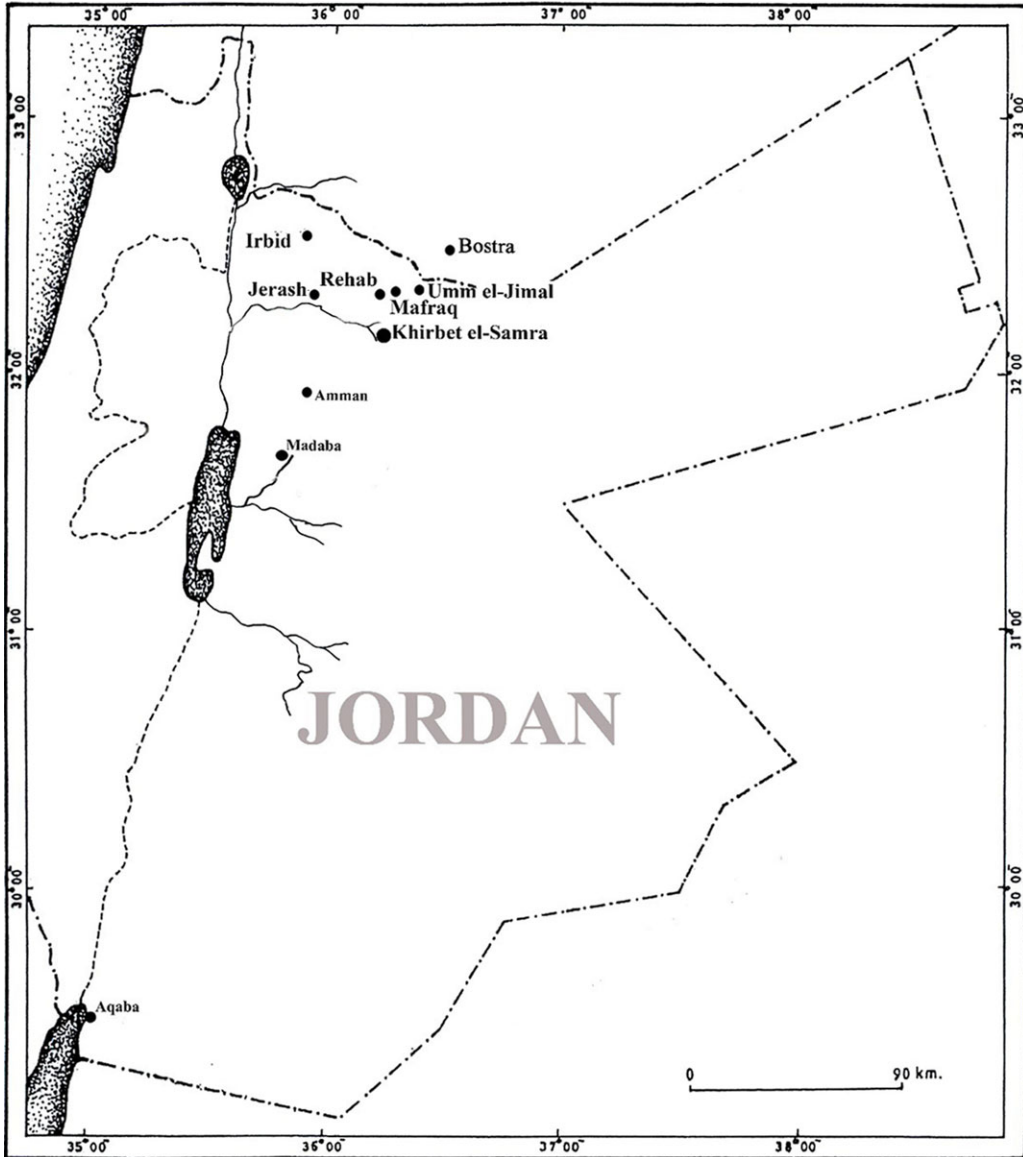*Corresponding author. Email: khaledsm@email.arizona.edu

Figure 1   Location map of Umm el-Jimal and sites mentioned in the paper.

buildings associated with them (the Church of Barracks, etc.) and names bearing on dedicatory or vow inscriptions found within them (Church of Julianus, Church of Numerianos, etc.).

Excluding the church of Julianus and the Cathedral, given specific dates by inscriptions out of context (reused inscribed lintels), the rest of the churches were assigned wider ranges of dates (4th or 5th or 6th and early 7th centuries) based on their architectural elements and styles and architectural comparisons with other dated churches in Syria (Butler 1929). De Vries (1985:251, 1998:230) dated the North East Church to ca. 490 AD and the Numerianos Church to a later year, and argued that most of the churches of Umm el-Jimal were probably built
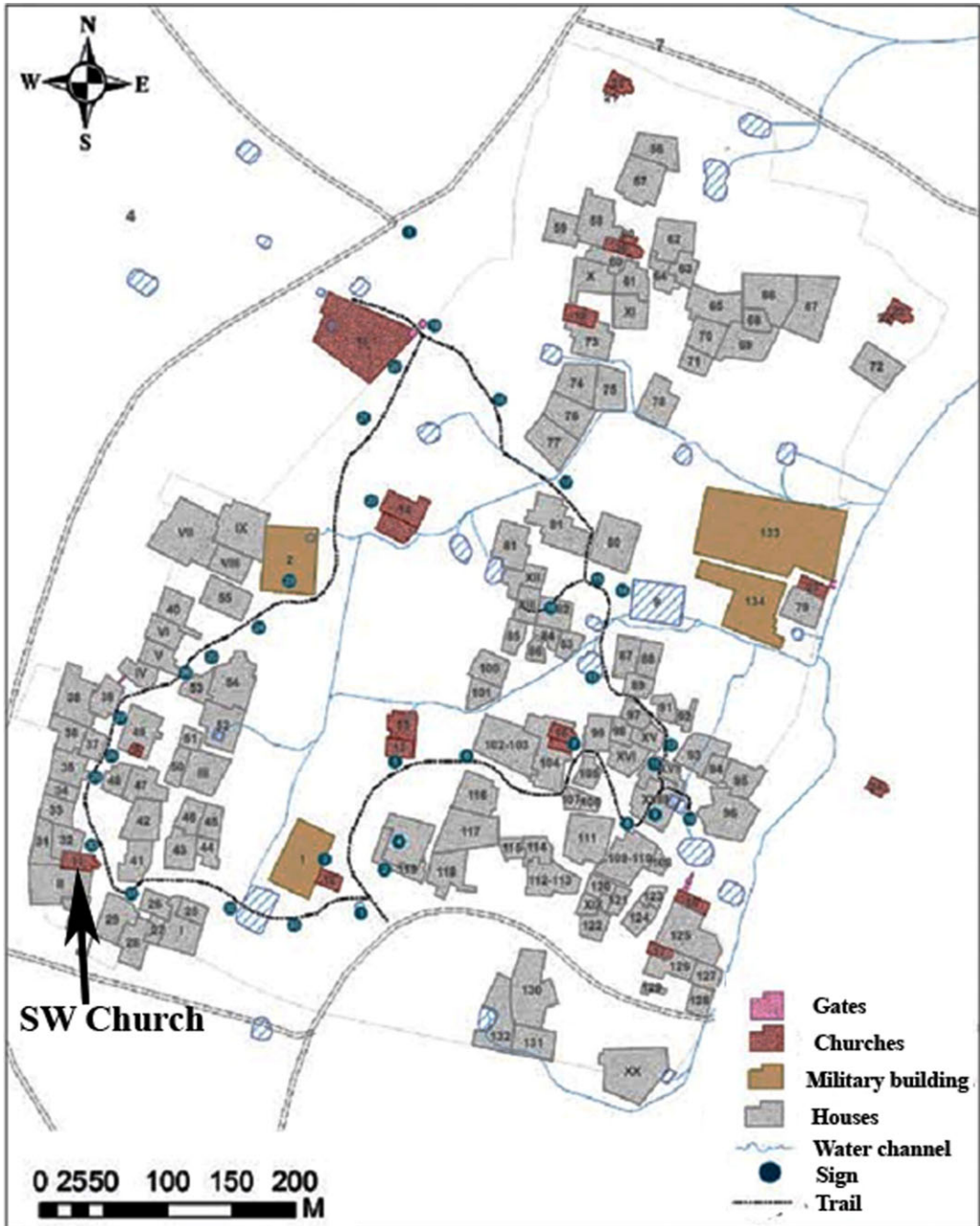
Figure 2 Umm el-Jimal, town plan, and location of the SW Church (after De Vries 2016).

during the prosperous late Byzantine period, as the many churches of the neighboring sites of Khirbet es-Samra, Rihab, Bostra, among others.

The churches of Umm el-Jimal, categorized into small hall churches and larger basilica churches, were constructed in different circumstances. Few churches are free standing

structures, while several of them were built against or inserted between older structures and house complexes which governed the distribution and size of their architectural elements, number and location of their doors, windows, etc. which makes it illogical to compare them with other churches built in different circumstances. Butler (1913:153) emphasized clearly that Umm el-Jimal buildings have the same lithic architectural forms, such as the corbel courses and roofing slabs in basalt, spread in the southern Hauran, but the ground plans and superstructures of its churches are of a greater variety than can be found in any other part of the Hauran, which covers the south part of Syria and north and northeastern parts of Jordan. In any case, specific dates have not been assigned for the establishments of the churches; therefore, it is unclear whether the churches were built contemporaneously or in successive intervals of time according to the growing number of its inhabitants and their demand for religious buildings and/or to replace destructed churches by natural disasters, mainly earthquakes.

One of the interesting features of the churches is their preservation of some cement materials, still *in situ* in some spots, used for filling the gaps between stone rows, or plastering the internal wall facades or bedding mosaics and floors. The cement materials have inclusions of organic materials mainly of charcoals, and straw in some cases, therefore this study will use the ^{14}C technique in dating the available organic inclusions of these materials i.e. the structures. Organic inclusions were used by Al-Bashaireh (2017) to date the mortar of the apse of the Umm el-Jimal Cathedral. He concluded that the measured radiocarbon date agrees with the date (557 AD) of the inscription found on the floor of the Cathedral. The radiocarbon dates of the charcoals uncovered from the mortar of the fallen dome of the West Church's apse assigned an early date (138–380 AD) for the dome (Al-Bashaireh 2016). In addition, Al-Bashaireh (2014) radiocarbon dated straw and charcoals from the plaster and mortar of the house XVII–XVIII and concluded that the house was plastered or built during the period between 425 and 535 AD, in the middle of the Byzantine period, in accordance with the conversion of the city to domestic uses. Furthermore, organic inclusions of mortar and plaster were used in dating several structures at Petra, Jordan (Al-Bashaireh and Hodgins 2011, 2012; Al-Bashaireh 2013) and churches in North of Jordan (Al-Bashaireh 2015).

This research is part of a large project aiming at the dating of the churches by archaeometric dating techniques, mainly radiocarbon. It aims to reconstruct the chronological sequence of the undated Southwest Church within its complex of houses and compare it to the chronology of other churches and the site in general. In addition, it aims to identify the main aspects of mortar recipes for the church at the time of their production.

The Southwest Church

The church is situated in the southwest part of the archaeological site, hence the name (Figure 2). It is a rectangular basilica formed of a semicircular apse, a chancel screen, and a nave flanked by two aisles which are delimited by two arcades of three arches each, see the plan of the church in Figure 3.

It had a flat roof where the two aisles were roofed with slabs of basalt (Butler 1913:183–184). The floor has incised decoration patterns that may have been drawn to guide the setting of the mosaic's tesserae. It was constructed adjacent to, and probably using the foundations and walls of, an existing complex of houses (houses 2 and 32). As a sequence of the attachment of the church to the complex, the entrances of the church are of peculiar locations: one in the south wall, two in the east wall (one on either side of the apse) and one in the north wall, Figure 3. The
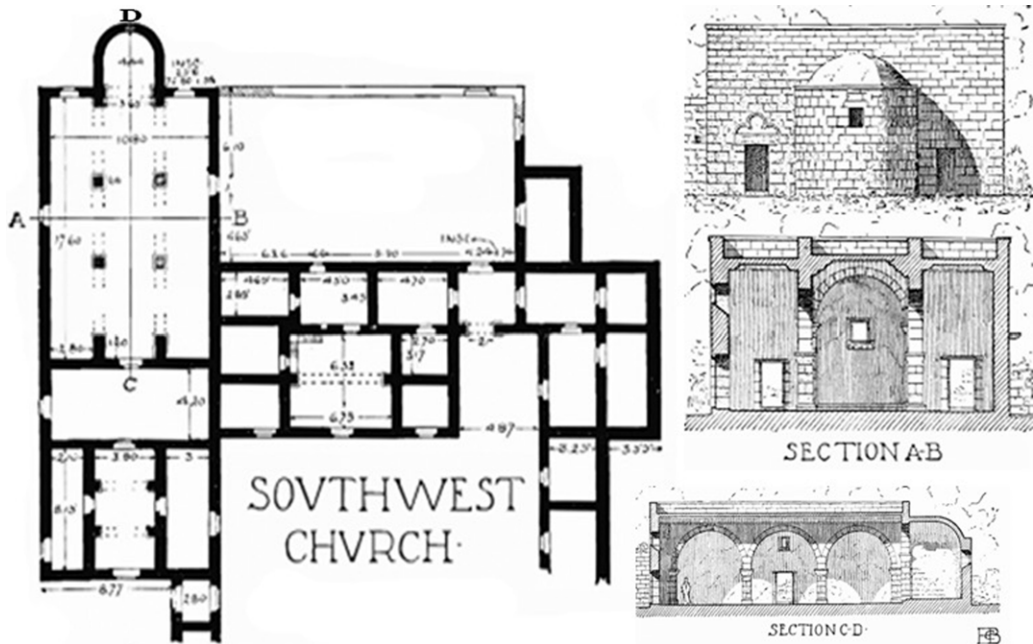
Figure 3   Plan of the Southwest Church (left), and reconstructions of the exterior the apse (upper right), and sections along A–B and C–D lines (Butler 1913:185).

church's southern wall clearly divides the church structure from the older complex, while its western wall has a door opening into an animal stable equipped with feeding mangers, though it was not the main entrance as other basilicas (Haddad 2019). However, it is not possible with the present data to decide whether the houses of the complex belonged to the church or kept their residential function after its establishment (Butler 1913:183).

The church was classified by Butler (1929:6) into a class II church: "the group of churches having three-aisles with longitudinal system of supports," type A "the churches that have a projecting apse without side chambers, and their naves are divided by two rows of three arches carried upon piers, two on either side with pilaster piers at either end"; accordingly, he dated it to the fifth century AD. As mentioned above, the excavations and clearance of the church in the past years showed that the church has only four main doors and not five as suggested by Butler (1929:41–43), therefore, this date of the church should be reconsidered. According to De Vries (1985:251, 1998:230) the church should be dated to the late Byzantine period. Coughenour (1987:24) classified the church as a "parish church" and dated it to the mid-sixth century AD based on two similar inscriptions carved on two lintels, used at that time, reading "Courage, fortune of the blues". The 1st lintel which has also a cross of western origin with the inscription was found in the church, while the 2nd lintel, has only the inscription, was found in one of the houses of the complex. It is possible that the cross is a later addition to the 1st lintel beside the inscription (at the time of building the church), therefore it might be dated after the mid-sixth century AD.

In any case, the above suggested dates are inconclusive and incompatible, therefore this research investigates the chronology of the church and examines the major characteristics of its mortars. After the clearance of the church in the past years, the Umm el-Jimal project (UJP)

Figure 4   The locations of the samples in the trenches, apse, collapsed arch, and north wall.

got the permission from the Department of Antiquities of Jordan, in 2017, to reopen the three pits dug by looters (see Figure 4) and collect cement materials from the pavement layers, the seat of west wall and the seat of the apse. The research was carried out to better understand the stratigraphy of the floor's pavement, radiocarbon date organic inclusions of the mortars to reconstruct the chronology of the church and determine the main recipes used in their production by archaeometric techniques.

MATERIALS AND METHODS

Materials

The three looters' trenches dug in the west part of the nave (trench1), east part of the south aisle (trench 2) and north part of the raised apse (trench 3) were excavated. It is worth mentioning that the excavations in trench 1 uncovered two floors, the upper at the surface and the second floor is about 40 cm deep (lower pavement) (Figure 4, upper left). The other two trenches have only the upper pavement.

Four bedding mortar samples were collected from the three trenches, two samples from the two floors of trench 1, one sample from the floor of trench 2, and one sample from the floor of trench 3. In addition, it was decided to collect jointing mortar samples left undisturbed *in situ* to radiocarbon date the apse's seat and the base of the west wall. One sample was collected from
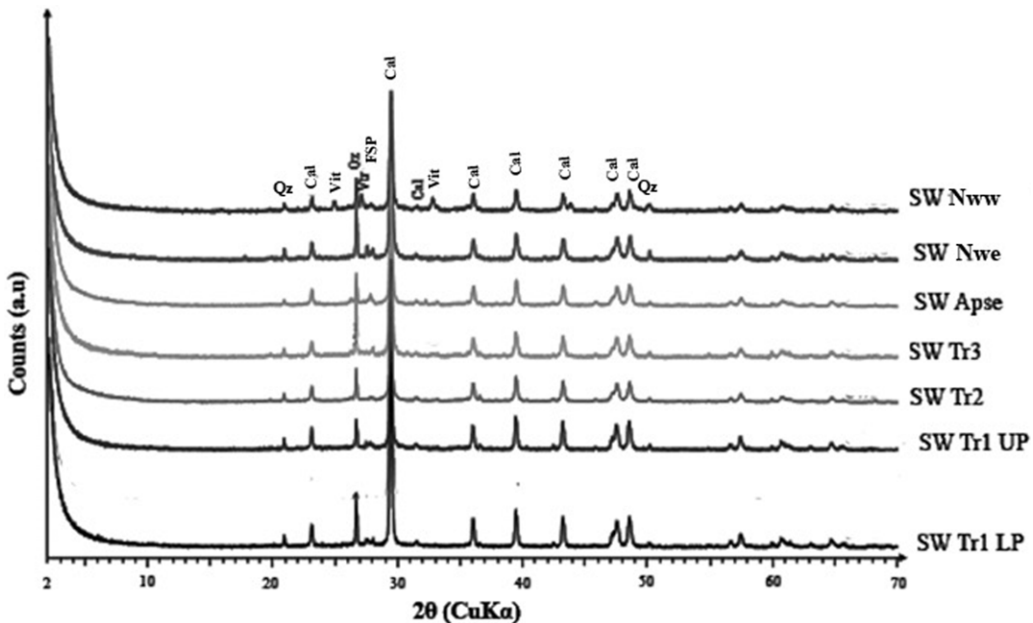
Figure 5 XRD spectra of the studied mortars of the SW Church (Qz quartz, Cal calcite, Vit Vaterite, FSP feldspar).

south part of the apse's seat and two samples from the base of the north wall (on the east and west sides of its door), to correlate its construction with the floor and the seat of the apse, especially that the south wall has a similar base. Seven charcoals were collected, one charcoal from each mortar sample. Furthermore, charcoal was uncovered underneath the stones of a collapsed arch which still *in situ* in front of the apse (Figure 6). Since the collapse of the arch approximates the time of the final destruction of the church, it was decided to radiocarbon date this charcoal to determine the time after which (*terminus post quem*) the arch collapsed.

Methods

The samples from the trenches were detached from intact mortars of the pavements, while the samples of the apse's seat and the base of the north wall were detached, after the removal of the surface material, by a hammer and a chisel from locations of original materials that did not show any disturbance or replastering, and most probably used in the initial construction. Parts of charcoal were seen by the naked eye in some samples, so a part of each sample was gently crushed and sieved to dissemble it and liberate the charcoals.

Fine thin rounded pieces were collected when available in search for charcoals of twigs or small branches that could overcome the old wood problem. The charcoals were pretreated and dated at the AMS facility of Klaus-Tschira-Labor für Physikalische Altersbestimmung, Curt-Engelhorn-Zentrum Archaeometrie gGmbH, Mannheim (code number MAMS). The samples were pre-treated using the ABA (acid/base/acid, HCl/NaOH/HCl) method, then insoluble fractions were used for further treatment. The treated samples were combusted to CO_2 in an Elemental Analyzer (EA), and the CO_2 was converted catalytically to graphite. ^{14}C was analyzed using a MICADAS (MIni CArbon DAting System, IonPlus) type AMS system
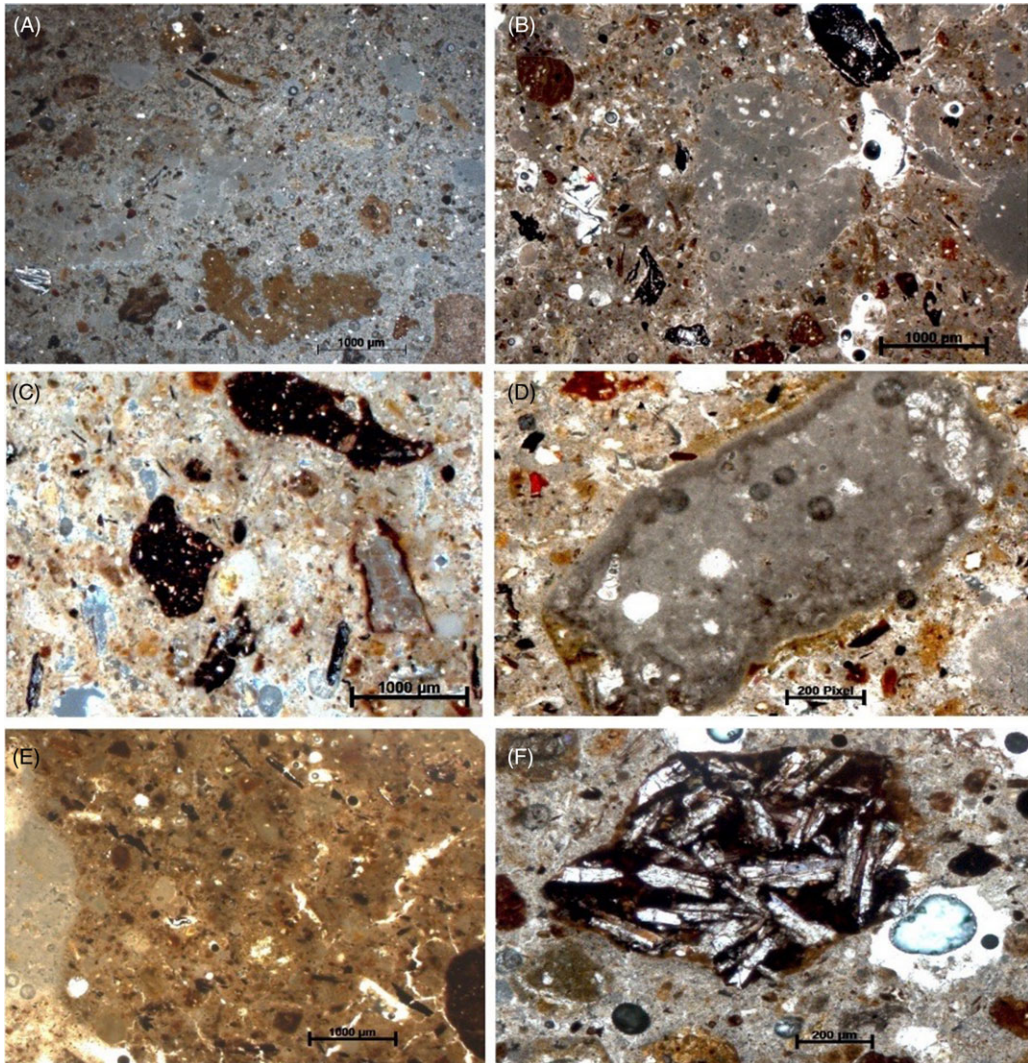
Figure 6   Microphotographs of the studied mortars showing the inclusions (A,B), in particular (A) nonhomogeneous matrix with lumps, (B) cracked lump (center), charcoal (black, upper center), (C) reaction rims of grogs, (D) under-burnt limestone grain with fossils, (E) irregular shapes of fissures through the mortar and around grains (bottom right), (F) plagioclase crystals in a volcanic inclusion.

in-house. The isotopic ratios $^{14}C/^{12}C$ and $^{13}C/^{12}C$ of samples, calibration standard (Oxalic Acid II), blanks and control standards were measured simultaneously in the AMS. ^{14}C-ages were normalized to $\delta^{13}C$=-25‰ (Stuiver and Polach 1977) and calibrated using the dataset IntCal20 and software OxCal 4.4, while calibration graphs were generated using the software OxCal (Reimer et al. 2020).

For the characterization of the samples, they were examined by the naked eye and a magnifying lens, and then characterized using X-ray diffraction (XRD) and thin-section petrography. The sieved fine powders were reacted with diluted hydrochloric acids. Powder diffraction patterns were obtained using a Bruker D8 advance equipped with a Cu-sealed tube (40kV/20mA), a

Göbel mirror optics, a 0.2 mm divergence slit, a fixed knife edge to suppress air scatter and a VÅNTEC 1-detector. The crystalline phases were identified using the pdf data from the 2006 International Centre for Diffraction Data-Joint Committee of Powder Diffraction Standards (ICDD-JCPDS).

Small blocks of samples were impregnated under vacuum with a low-viscosity epoxy resin until their solidification (Elsen 2006:1417–1418). The solid blocks were used to produce thin sections, one side of the block was carefully polished and then mounted on to a microscope slide. Afterwards, the thickness of the block was reduced by sawing off the material and polishing it until the resulting thin section was about 30 μm thick. The thin sections were examined using a Zeiss Axioskop 40 polarized light microscope with digital imaging system Zeiss AxioVision (at the Curt-Engelhorn-Centre of Archaeometry, CEZA, Mannheim, Germany).

RESULTS AND DISCUSSION

Characterization of the Mortars

Cement materials (plaster, mortar, concrete) are made of a binder (lime, gypsum, or mud) mixed with inclusions of organic (wood, straws, charcoal, etc.) and inorganic (sand and crushed rocks, ceramic, etc.) origin.

Macroscopic examination showed that the samples under investigation are gray in color due to their content of charcoal. The upper and lower mortar layers of the first trench are thin, while the lower one is about 15 cm thick. The samples comprise rounded white lime lumps and some coarse-grained volcanic inclusions seen by naked eyes. They showed a moderate hardness and a fair cohesion.

The addition of diluted hydrochloric acid to the fine powders of the mortars produced a reaction with bubbles, indicating that chemical composition of the powder is calcium carbonate (calcite).

X-Ray Diffraction Analysis

The XRD results showed that the investigated mortars are similar in their mineralogical composition. The spectra, in Figure 5, show the presence of the major component of calcite, minor components of quartz and feldspar, and traces of other phases of calcium carbonates; aragonite (in samples SW Tr.2, SW Tr.3, SW Apse) and vaterite (in sample SW Nww).

XRD results are in accordance with the simple diluted acid test indicating that the mortars are lime-based, where calcium carbonate or calcite is their binding agent. Therefore, the calcite of the binder is the major contributor to the high peak of calcite in the spectra, while the limestone inclusions represent another, but minor, source of the calcite. The inclusions are the sources of the other mineral phases of quartz, feldspars, and partially the calcite, while aragonite and vaterite carbonate phases were most probably formed in the pore spaces of the mortars under certain conditions of temperature and pressure (Haneefa et al. 2019:545–548; Rodriguez-Blanco et al. 2011:270). In general, the presence of highly supersaturated solutions of Ca^{2+} and CO_3^{2-} ions in the mortar voids and pore spaces precipitate in different carbonate mineral phases; vaterite at low temperatures between 14 and 30ºC and aragonite at higher ones between 60 and 80ºC (Ogino et al. 1987).

Table 1 ^{14}C ages, calibrated ages, and the δ^{13}C values of the dated charcoals from the SW Church.

S. Lab. # MAMS	S. ID	^{14}C age ± s.d. (yr BP)	Calibrated ages Cal AD		δ^{13}C AMS (‰)	Material
			68.3%	95.4%		
51757	SW Tr1.UP	1471 ± 14	583–636	570–640	–25.6	Charcoal
51758	SW Tr1.LP	1606 ± 14	424–532	419–537	–22.9	Charcoal
51756	SW Tr2	1479 ± 14	575–604	566–638	–10.9	Charcoal
51755	SW Tr3	1440 ± 14	605–641	600–646	–23.6	Charcoal
51761	SW Apse	1439 ± 13	606–642	600–646	–16.5	Charcoal
51760	SW Nww	1702 ± 24	265–404	258–414	–33.6	Charcoal
51762	SW Nwe	1653 ± 16	404–424	267–529	–28.1	Charcoal
57404	Collapsed arch	989 ± 23	1021–1123	995–1154	–2.9	Charcoal

Petrographic Examination

Petrographic examination showed nonhomogeneous brown to gray colored fine matrices comprising fissures, some are partially filled with recrystallized calcite lime, and lime lumps with cracks (Figure 6A,B). The shrinkage of the lime during setting and slaking most probably produced the cracks and fissures, while the irregular shaped fissures are a post depositional dissolution of the binder (Figure 6E) (Leslie and Hughes 2002; Elsen 2006; Elsen et al. 2011). The presence of the lumps is attributed to different reasons including dry slaking which uses the minimum amount of water to slake the quicklime, incomplete slaking, insufficient mixing, or hot mixing (Bakolas et al. 1995; Callebaut et al. 2001; Degryse et al. 2002).

The most abundant inclusions of the mortars are charcoals (20–30%) and crushed ceramics (grog) (10–25%) (Figure 6A, and the less abundant inclusions are old mortar (5–15%), limestone (5–15%), quartz (3–10%), volcanic inclusions (5–10%), and iron oxides (3–10%) (Figure 6). Limestone and quartz are mostly subrounded, while crushed grogs and volcanic grains are angular to subrounded. Under-burnt limestone grains having fossils and/or fossil ghosts (Figure 6D) most probably resulted from incomplete or low firing temperatures (Hughes and Cuthbert 2000; Lezzerini et al. 2017; Ergenc et al. 2021). The mortar content of natural (inclusions of volcanic origin) (Figure 6F) and artificial (crushed ceramics) pozzolanic materials are usually used to produce hydraulic properties for the mortar, which forms good contacts with the binder and enhances the strength and durability of the mortar (Arizzi and Cultrone 2021, see the reaction rim of the binder and a ceramic in Figure 6C). The estimated binder: aggregate (b:a) ratios, visually estimated on thin sections by comparison with standard charts used by sedimentologists, ranged between 1:3 and 1:4. This range follows the recommended a:b ratios used in ancient Roman mortars (Lechtman and Hobbs 1987).

Radiocarbon Dating

The ^{14}C ages, calibrated ages, and the δ^{13}C values of the charcoals are reported in Table 1 and illustrated in Figure 7. It is worth mentioning that the δ^{13}C values are measured with an AMS system to serve as a measure for the fractionation that occurred during preparation or analysis. Therefore, they are not suitable for interpretation as would be the case for measurement with a stable isotope measurement.
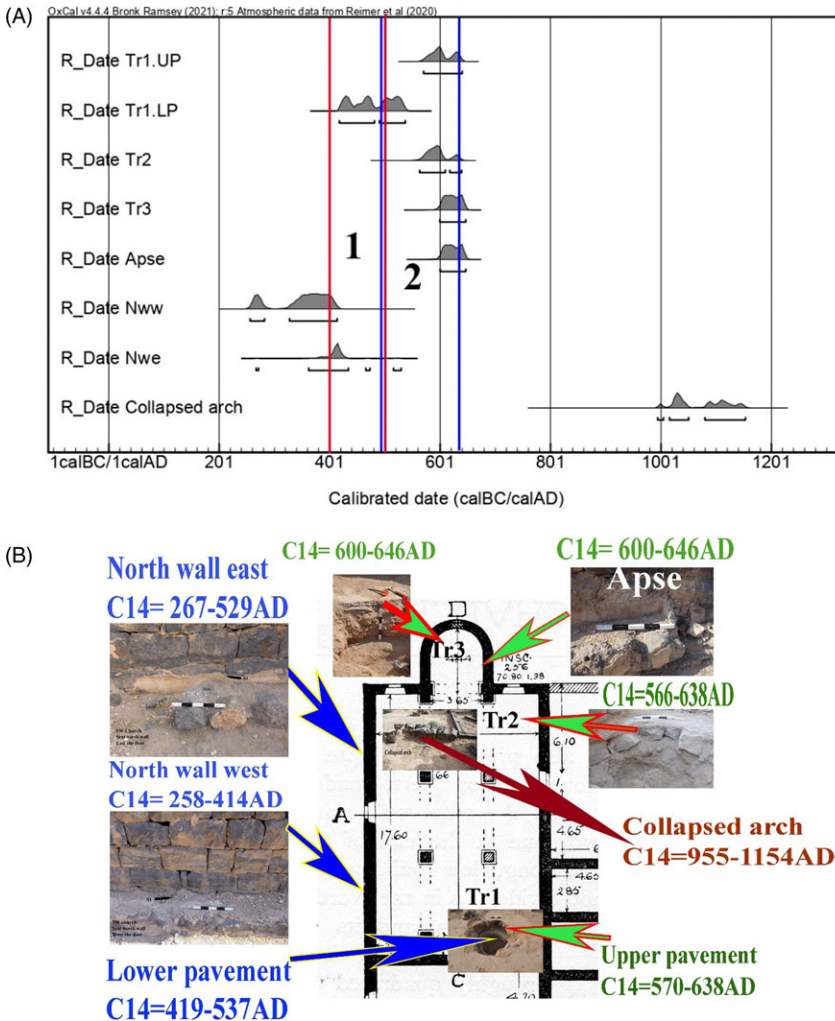
Figure 7 (Top) OxCal plot of all ^{14}C dates of the charcoals of the SW church arranged according to the building elements sampled and compared to the suggested archaeological dates of Butler (1) and De Vries (2). (Bottom) Location of the trenches and samples on the church's plan and their ^{14}C calibrated dates (95.4%), the blue color represents the 1st phase of construction of the complex (base of the west wall and the lower pavement of trench 1), the green color represents the 3rd phase after the 2nd phase of destruction by the 551 earthquake (the pavements of the trenches 2 and 3, the upper pavement of trench 1, and the seat of the apse), the red color represents the final collapse of the church after the 749 earthquake. (Please see online version for color figures.)

The ^{14}C age of the floor of the church's hall was determined by radiocarbon dating the nave's pavement (trench 1, upper pavement) and the southern aisle's pavement (trench 2), see Figure 4. These two radiocarbon dates at 95.4% (all the calibrated ages in this section are at 95.4%) are alike (570–640 AD and 566–638 AD) (Figure 7). The radiocarbon ages of the floor of the apse (trench 3) and the seat of the apse are identical (600–646 AD). All of these dates fall within the period between 566 and 646 AD, within the late Byzantine period (490–636 AD) (Figure 7).
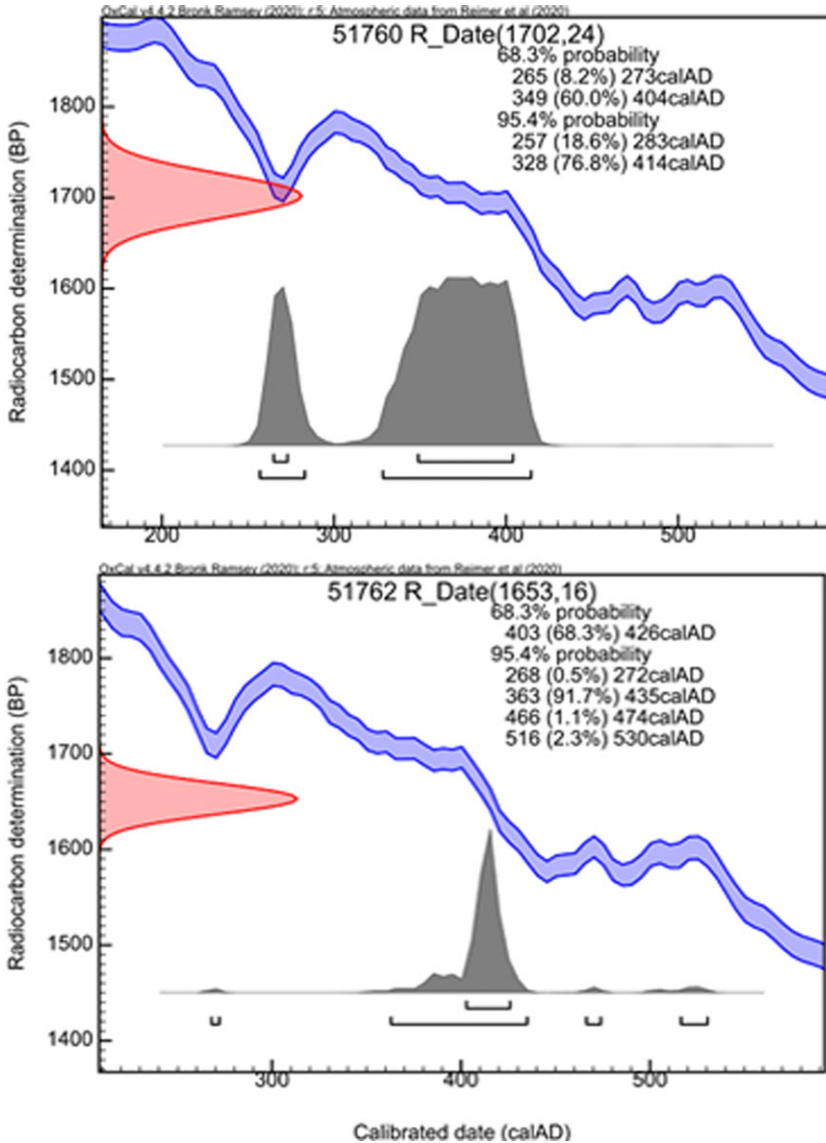
Figure 8 The ¹⁴C dates of the north wall's mortars.

In contrast, the radiocarbon date of the lower pavement of trench 1 (419–537 AD) is older than the age of the upper pavement, without any overlap. The two radiocarbon dates of both parts of the base of the north wall (west the door 258–414 AD and east the door 267–529 AD) are also older than the church floor i.e., upper pavement, without overlapping as well (Figure 8). However, when these ages are compared to that of the lower pavement, the west part of the base is older (without overlap), while the age of the east part embraces most of the radiocarbon date of this pavement. It is likely that the wall, and the whole house complex, were built during the early Byzantine period in accordance with time given by De Vries (1985, 1990, 1998) for the conversion of the site into domestic uses.
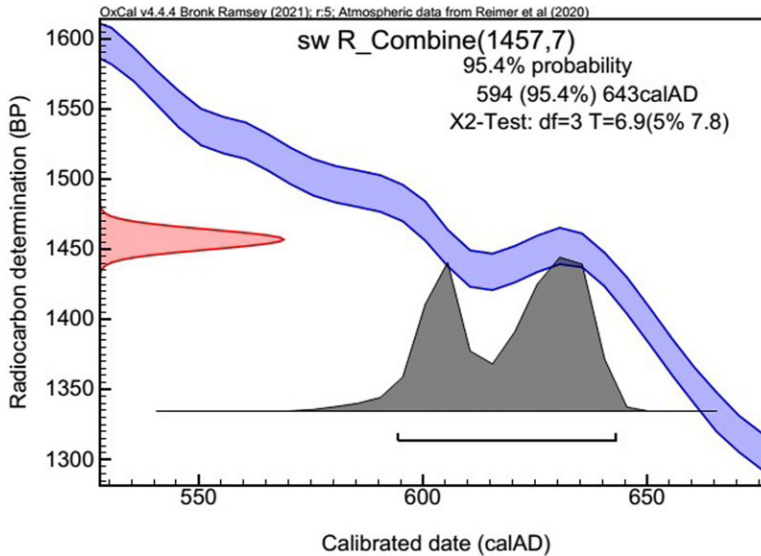
Figure 9 Combined ^{14}C age of all ^{14}C measured dates of the SW Church's floor and the apse seat.

For the date of the arch collapse, the ^{14}C determination showed an age (995–1154 AD) younger than expected. It is agreed that most of the Umm el-Jimal structures were heavily damaged and many of them were destroyed by the 749 major earthquake. The devasting 749 earthquake, of a magnitude of 7, heavily affected Palestine, Jordan, Lebanon, Syria and other cities in the Levant (Russell 1985). It is very possible that the arch, and probably other parts of the church, were weakened by the earthquake but survived till the time they could not withstand more and collapsed sometime after 995 AD by itself or one of the many earthquakes that hit the region, see Amiran et al. 1994 and Zohar et al. 2016, among others, for more information.

Figure 4 shows that the large basalt stones of the first preparatory layer (*statumen*) of the eventual church floor were laid in the whole area, and directly on the lower floor which lacks any foundation or preparatory layers. Therefore, it is very unlikely that the lower floor belongs to an older church that was refurbished. More likely, it belongs to a courtyard of the houses and was confined by the north wall and an east one in the same position of the existing east wall. The church was buttressed in this space against the south and west walls of the houses, and most probably utilized the base of the north wall (De Vries, personal communication; Rohl 2019).

The similar dates of the pavements of trench 1 and trench 2 indicate that the floor was laid during this time period. The overlap of these two dates with the identical two dates of the apse's raised pavement and the seat indicates that the final stage of flooring the whole church and plastering of the apse most probably happened during first four decades of the seventh c. AD. However, assuming that the above four dates represent the same event, their combined date 594–643 AD (Figure 9) should be the probable age for the construction of the church.

Compiling these dates shows that the church and the architectural elements associated with it passed through different construction, paving, plastering, destruction and abandonment phases as suggested in Table 2 and Figure 10.

Table 2   Suggested construction, destruction and abandonment phases for the SW Church.

Phase	Event	Date	Source of evidence
1	Construction of older walls and pavement	267–529 AD	North wall and lower pavement in trench 1
2	Earthquake destruction	551 AD	Pause of construction events, and historical record
3	Church's construction, paving the floors and plastering	566–646 AD	Trenches 1, 2, 3 and apse's seat
4	Earthquake destruction and abandonment	After 749 AD	Historical record
5	Final collapse	After 995–1154 AD	Arch collapse

The 1st phase was a construction and occupational one before the destruction phase (phase 2) of 551 AD earthquake. The 3rd phase that occurred after 551 AD was a phase of construction, paving the floors and plastering the walls and apse. It was followed by a destruction and abandonment phase (phase 4) caused by the 749 AD earthquake. The 5th phase was the final collapse of the church, probably after 995–1154 AD.

CONCLUSIONS

The research investigated the chronology of the Southwest Church which was most probably built in yard of a complex of Byzantine houses making use of some of their walls and floor. In this research, AMS radiocarbon dated organic inclusions uncovered from the bedding mortars of the floors and the jointing mortars of the seat of the apse and base of the north wall of the Southwest Church. The measured dates enabled the reconstruction of the most probable chronology of the building stages of the church and its associated complex. While the first flooring of an ancient structure (probably a yard) and the base of the north wall took place probably in the late 4th to early 5th c. AD, flooring and plastering of the church took place most probably in the period between the very end years the 6th c. and the first four decades of the 7th c. AD. The church, like the whole site, was most probably affected by and abandoned after the devasting earthquake of 749 AD. Furthermore, the radiocarbon dates suggest a final collapse starting probably from 995 AD.

The late date for the construction of the church is unsurprising, several churches were constructed, in sites not far from Umm el-Jimal, during the same period. For instance, at Khirbet as-Samra, the church of Saint George (637 AD); at Rehab, many of its 31 churches were built after 590 AD including, among others: the church of Saint Basil and Procopius (594 AD), the church of Saint Peter (623 AD), the church of Saint Menas (635 AD), the church of John the Baptist church (619 AD), at Gerasa the church of the bishop of Genesius (611 AD) (Kraeling 1938; Lux 1967; Piccirillo 1980, 1993; Humbert 1990; Aliquot and Al-Husan 2020); and examples of churches built during the Umayyad period see Piccirillo (1984).

The placement of the church between a complex of houses, its floor without mosaic, low quality of finishing, building on ancient walls that do not provide true right angles, modified plan and difference in its dimensions (Haddad 2019:89), do not indicate a prosperous period of Umm el-Jimal. It is very possible that its community suffered the earthquake of 551 AD, plague and
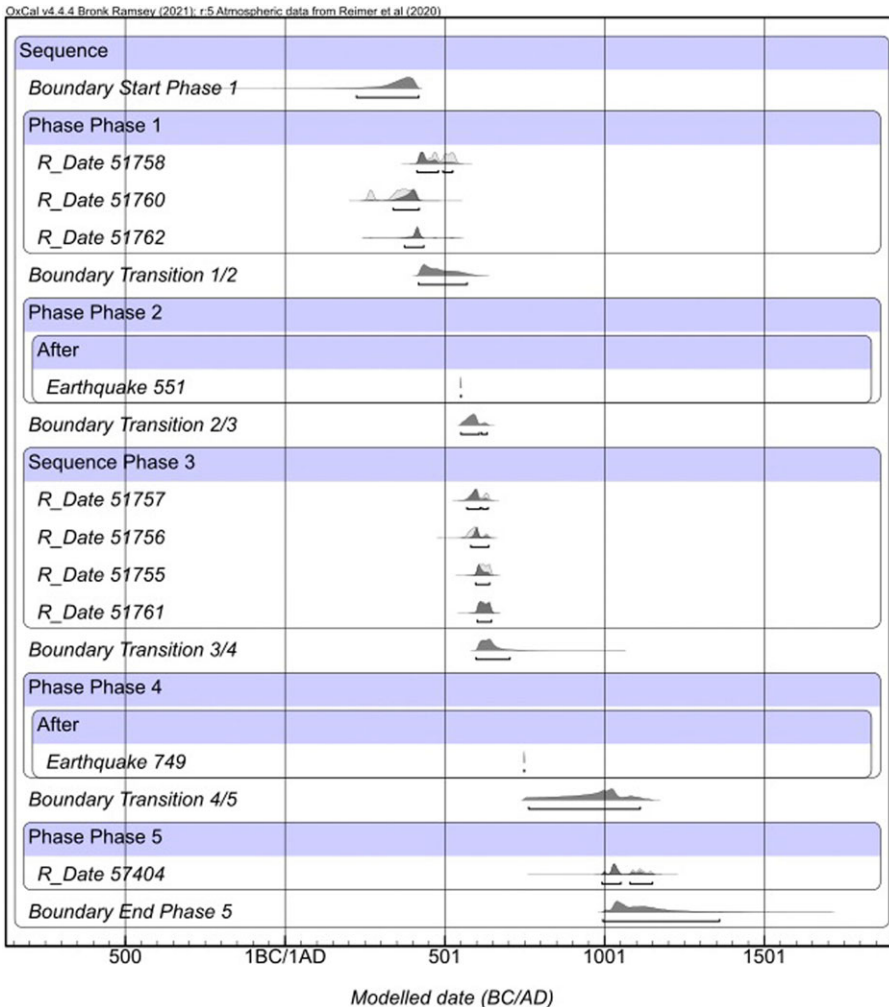
Figure 10 An Oxcal Bayesian model highlighting the suggested 5 phases of construction, destruction and abandonment and final collapse occurred during the history of the church (model by Ronny Friedrich, Curt-Engelhorn-Zentrum Archäometrie gGmbH CEZA), the boundaries (B) of the phases (Ph) of the model are the following: Boundary Start Phase 1: 224–419 AD, Boundary Transition (BT) 1/2: 419–570 AD, BT 2/3: 551–633 AD, BT 3/4: 599–703 AD, BT 4/5: 763–1112 AD, B End Ph.5: 996–1364.

Persian wars during the late 6th c. AD, therefore the weakened community could not afford the expenses of building luxurious or higher quality new free-standing churches.

The results of the characterization of the samples indicate that the mortar production at Umm el-Jimal relied on local raw materials of the city and its vicinity. The results show that the mortars regardless their function, bedding or jointing, have the same aggregates that differ slightly in their amounts; therefore, their production followed the same recipe. Although the samples were produced following the recommended 1:3, b:a ratio, insufficient mixing and firing indicate an imperfect technology. The continuous use of the same mortar recipe during a long time period between the third or fourth c. AD to the end of the sixth-early seventh centuries AD indicates an inherited production technology of mortar for generations.

ACKNOWLEDGMENTS

REFERENCES

Al-Bashaireh K. 2014. Reconstructing the chronology of the house XVII–XVIII complex at Umm El-Jimal, east Jordan: radiocarbon dates of organic inclusions of architectural mortars. Radiocarbon 56(1):245–256.

Al-Bashaireh K. 2015. Radiocarbon age determinations of mosaic mortar layers of churches from North Jordan. Radiocarbon 57(5):851–863.

Al-Bashaireh K. 2016. Use of lightweight lime mortar in the construction of the west church of umm el-Jimal, Jordan: radiocarbon dating and characterization. Radiocarbon 58(3):583–598.

Al-Bashaireh K. 2017. Umm el-Jimal cathedral, Jordan: inscriptions and radiocarbon dates. Arabian Archaeology and Epigraphy 28(1):61–66.

Al-Bashaireh K. 2013. Plaster and mortar radiocarbon dating of Nabatean and Islamic structures, South Jordan. Archaeometry 55(2):329–354.

Al-Bashaireh K, Hodgins GW. 2011. AMS ^{14}C dating of organic inclusions of plaster and mortar from different structures at Petra-Jordan. Journal of Archaeological Science 38(3):485–491.

Al-Bashaireh K, Hodgins GW. 2012. Lime mortar and plaster: a radiocarbon dating tool for dating Nabatean structures in Petra, Jordan. Radiocarbon 54(3–4):905–914.

Al-Shorman A, Ababneh A, Rawashdih A, Makhadmih A, Alsaad S, Jamhawi M. 2017. Travel and hospitality in late antiquity: A case study from Umm El-Jimal in eastern Jordan. Near Eastern Archaeology 80(1):22–28.

Aliquot J, Al-Husan AQ. 2020. The church of Saint John the Baptist in Riḥāb (Jordan): epigraphy and history. Berytus 59:107–130.

Amiran D. H, Arieh E, Turcotte T. 1994. Earthquakes in Israel and adjacent areas: Macroseismic observations since 100 BCE. Israel Exploration Journal 260–305.

Arizzi A, Cultrone G. 2021. Mortars and plasters—how to characterise hydraulic mortars. Archaeological and Anthropological Sciences 13(9):144.

Bakolas A, Biscontin G, Moropoulou A, Zendri E. 1995. Characterization of the lumps in the mortars of historic masonry. Thermochimica Acta 269:809–816.

Butler HC. 1913. Ancient Architecture in Syria, Southern Syria: Umm Idj-Djmâl. Division II. Leiden: Brill.

Butler HC. 1929. Early churches in Syria: fourth to seventh centuries. Amsterdam: Hakkert.

Callebaut K, Elsen J, Van Balen K, Viaene W. 2001. Nineteenth century hydraulic restoration mortars in the Saint Michael's Church (Leuven, Belgium): natural hydraulic lime or cement? Cement and Concrete Research 31(3):397–403.

Coughenour RA. 1987. The fifteen churches of Umm el-Jimal [unpublished manuscript]. Holland, MI: Western Theological Seminary.

De Vries B. 1979. Research at Umm el-Jimal, Jordan, 1972–1977. The Biblical Archaeologist 42(1): 49–55.

De Vries B. 1985. Urbanization in the basalt region of north Jordan in late antiquity: the case of Umm el-Jimal. Studies in the history and archaeology of Jordan 2: 249–256.

De Vries B. 1990. Umm el-Jimal: "Gem of the Black Desert"; a brief guide to the antiquities. Al Kutba, Amman.

De Vries B. 1993. The Umm el-Jimal Project, 1981–1992. Annual of the Department of Antiquities of Jordan 37:433–460.

De Vries B. 1994. What's in a name: the anonymity of ancient Umm el-Jimal. Biblical Archaeologist 57(4):215–219.

De Vries B. 1998. Umm el-Jimal: a frontier town and its landscape in northern Jordan. Volume I. Journal of Roman Archaeology, Supplementary Series no. 26.

De Vries B. 2016. Archaeology for the Future at Umm el-Jimal: site preservation, presentation, and community engagement. Newsletter of the American Center of Oriental Research 28(1):1–5.

Degryse P, Elsen J, Waelkens M. 2002. Study of ancient mortars from Sagalassos (Turkey) in view of their conservation. Cement and Concrete Research 32(9):1457–1463.

Elsen J. 2006. Microscopy of historic mortars—a review. Cement and Concrete Research 36(8): 1416–1424.

Elsen J, Mertens G, Van Balen K. 2011. Raw materials used in ancient mortars from the Cathedral of Notre-Dame in Tournai (Belgium). European Journal of Mineralogy 23(6):871–882.

Ergenc D, Fort R, Varas-Muriel MJ, Alvarez de Buergo M. 2021. Mortars and plasters—how to characterize aerial mortars and plasters. Archaeological and Anthropological Sciences 13(11):197.

Glueck N. 1942. Nabatean Syria. Bulletin of the American Schools of Oriental Research 85(1): 3–8.

Haddad M. 2019. A paradigm for local ecclesiastical architecture in Jordan, comparative study of three churches at Umm el-Jimal [unpublished master's thesis]. The University of Jordan.

Haneefa KM, Rani SD, Ramasamy R, Santhanam M. 2019. Microstructure and geochemistry of lime plaster mortar from a heritage structure. Construction and Building Materials 225:538–554.

Hughes JJ, Cuthbert SJ. 2000. The petrography and microstructure of medieval lime mortars from the west of Scotland: Implications for the formulation of repair and replacement mortars. Materials and Structures 33:594–600.

Humbert JB. 1990. Khirbet es-Samra du diocèse de Bosra. Christian Archaeology in the Holy Land: New Discoveries; Essays in Honour of Virgilio C. Corbo, OFM:467–474.

Kraeling CH. 1938. Gerasa. City of the Decapolis. An account embodying the record of a joint excavation conducted by Yale Univ. and the British School of Archaeology in Jerusalem (1928–1930), and Yale Univ. and the American School of oriental Research (1930–31, 1933–34).

Lechtman HN, Hobbs LW. 1987. Roman concrete and the Roman architectural revolution. In: High-technology ceramics: past, present, and future. The Nature of Innovation and Change in Ceramic Technology 3:81–128.

Leslie AB, Hughes JJ. 2002. Binder microstructure in lime mortars: implications for the interpretation of analysis results. Quarterly Journal of Engineering Geology and Hydrogeology 35(3):257–263.

Lezzerini M, Ramacciotti M, Cantini F, Fatighenti B, Antonelli F, Pecchioni E, et al. 2017. Archaeometric study of natural hydraulic mortars: the case of the Late Roman Villa dell'Oratorio (Florence, Italy). Archaeological and Anthropological Sciences 9:603–615.

Lux U. 1967. Der Mosaikfußboden der Menas-Kirche in Riḥāb. Zeitschrift des Deutschen Palästina-Vereins (1953-), (H. 1):34–41.

Ogino T, Suzuki T, Sawada K. 1987. The formation and transformation mechanism of calcium carbonate in water. Geochimica et Cosmochimica Acta 51(10):2757–2767.

Piccirillo M. 1980. Le antichità di Rihab dei Bene Hasan. Liber annuus. Studii Biblici Franciscani Jérusalem 30:317–350.

Piccirillo M. 1984. The Umayyad Churches of Jordan. Annual of the Department of Antiquities 28: 333–341.

Piccirillo M. 1993. The Mosaics of Jordan. Amman: American Center for Oriental Research.

Reimer PJ, Austin WE, Bard E, Bayliss A, Blackwell PG, Ramsey CB, et al. 2020. The IntCal20 Northern Hemisphere radiocarbon age calibration curve (0–55 cal kBP). Radiocarbon 62(4):725–757.

Rodriguez-Blanco JD, Shaw S, Benning LG. 2011. The kinetics and mechanisms of amorphous calcium carbonate (ACC) crystallization to calcite, via vaterite. Nanoscale 3(1):265–271.

Rohl DJ. 2019. Umm el-Jimal Project 2019 Excavations. Unpublished report submitted to the Department of Antiquities of Jordan.

Russell KW. 1985. The earthquake chronology of Palestine and northwest Arabia from the 2nd through the mid-8th century AD. Bulletin of the American Schools of Oriental Research 260(1): 37–59.

Stuiver M, Polach HA. 1977. Discussion reporting of ^{14}C data. Radiocarbon 19(3):355–363.

Zohar M, Salamon A, Rubin R. 2016. Reappraised list of historical earthquakes that affected Israel and its close surroundings. Journal of Seismology 20:971–985.